

Fig. 35A-20-001. KTiOAsO_4 . Typical morphology of crystals grown from the tungstate flux [91Che].

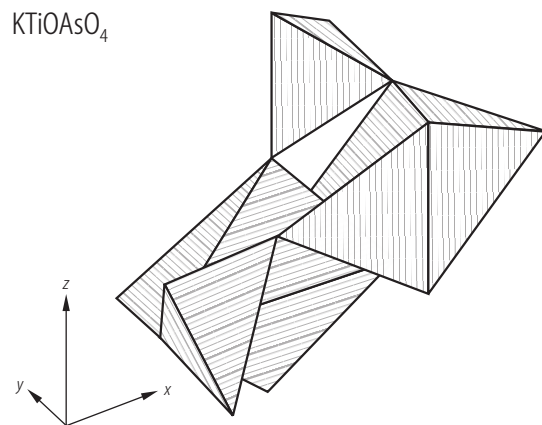


Fig. 35A-20-002. KTiOAsO_4 . Schematic representation of the basic structure $(\text{TiO}_6 - \text{AsO}_4)_2$ [86ElB].

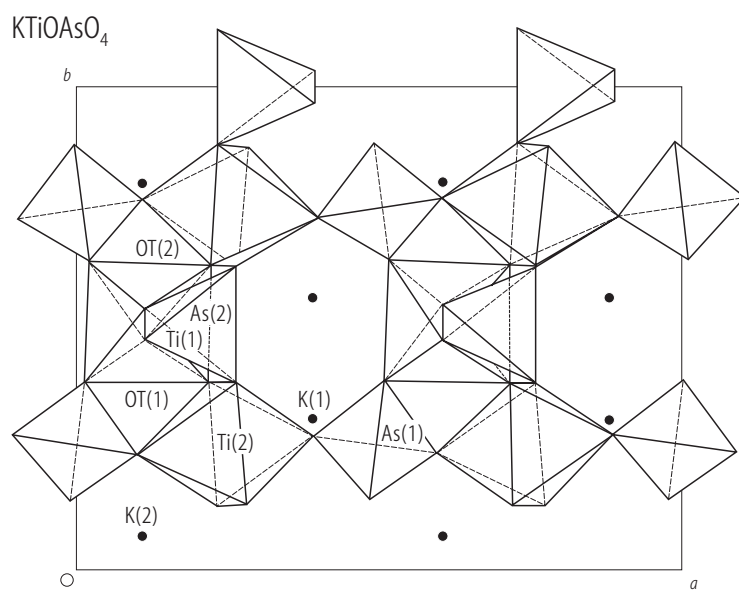


Fig. 35A-20-003. KTiOAsO_4 . Projection of the structure on the c -plane [86ElB].

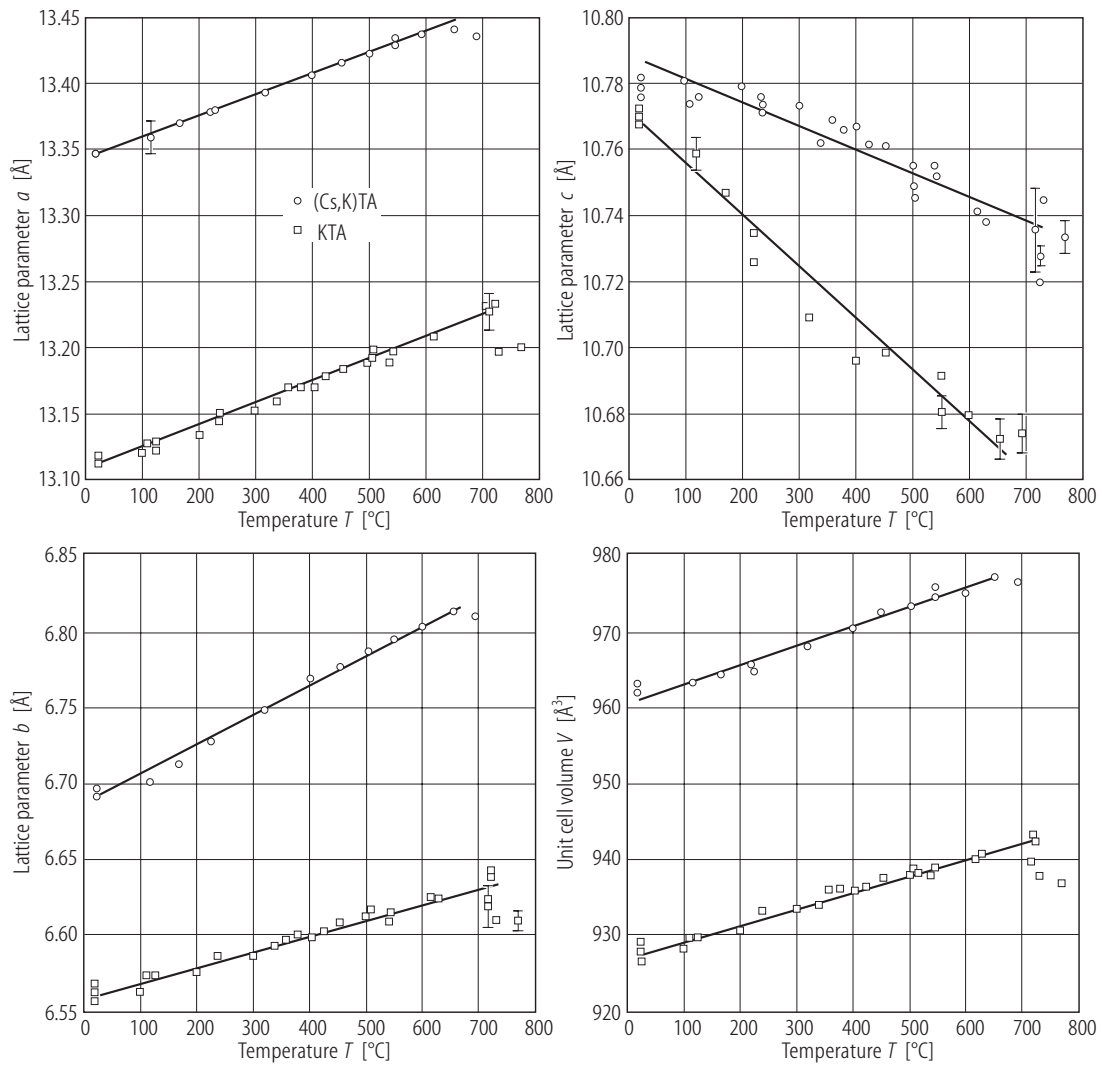


Fig. 35A-20-004. KTiOAsO_4 , $\text{Cs}_{0.6}\text{K}_{0.4}\text{TiOAsO}_4$. a , b , c and V vs. T [94Nor]. V : unit cell volume.

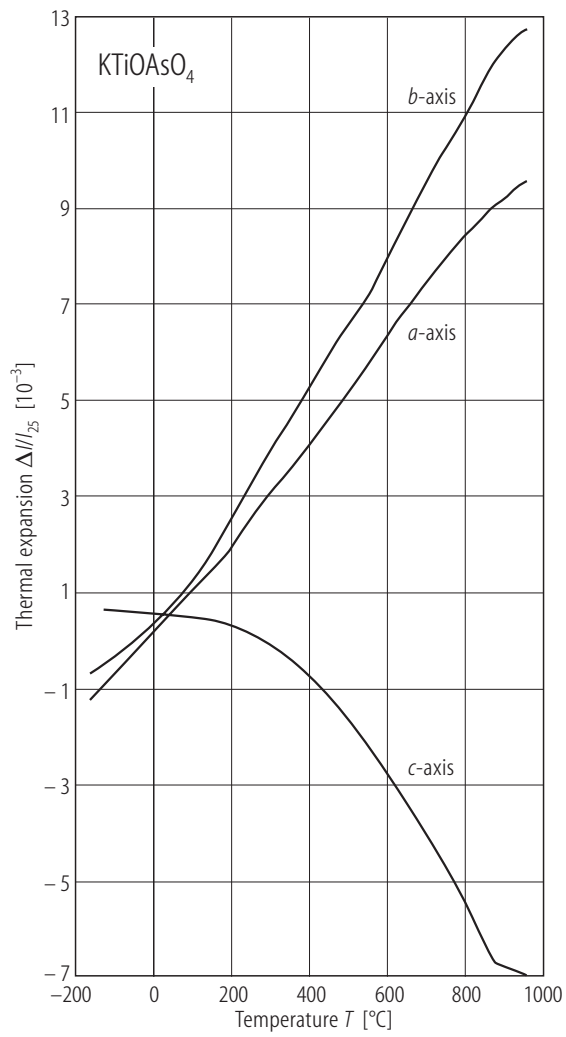


Fig. 35A-20-005. KTiOAsO_4 . $\Delta l/l_{25}$ vs. T [94Zho]. $\Delta l/l_{25}$: fractional thermal expansion in reference to 25 $^{\circ}\text{C}$.

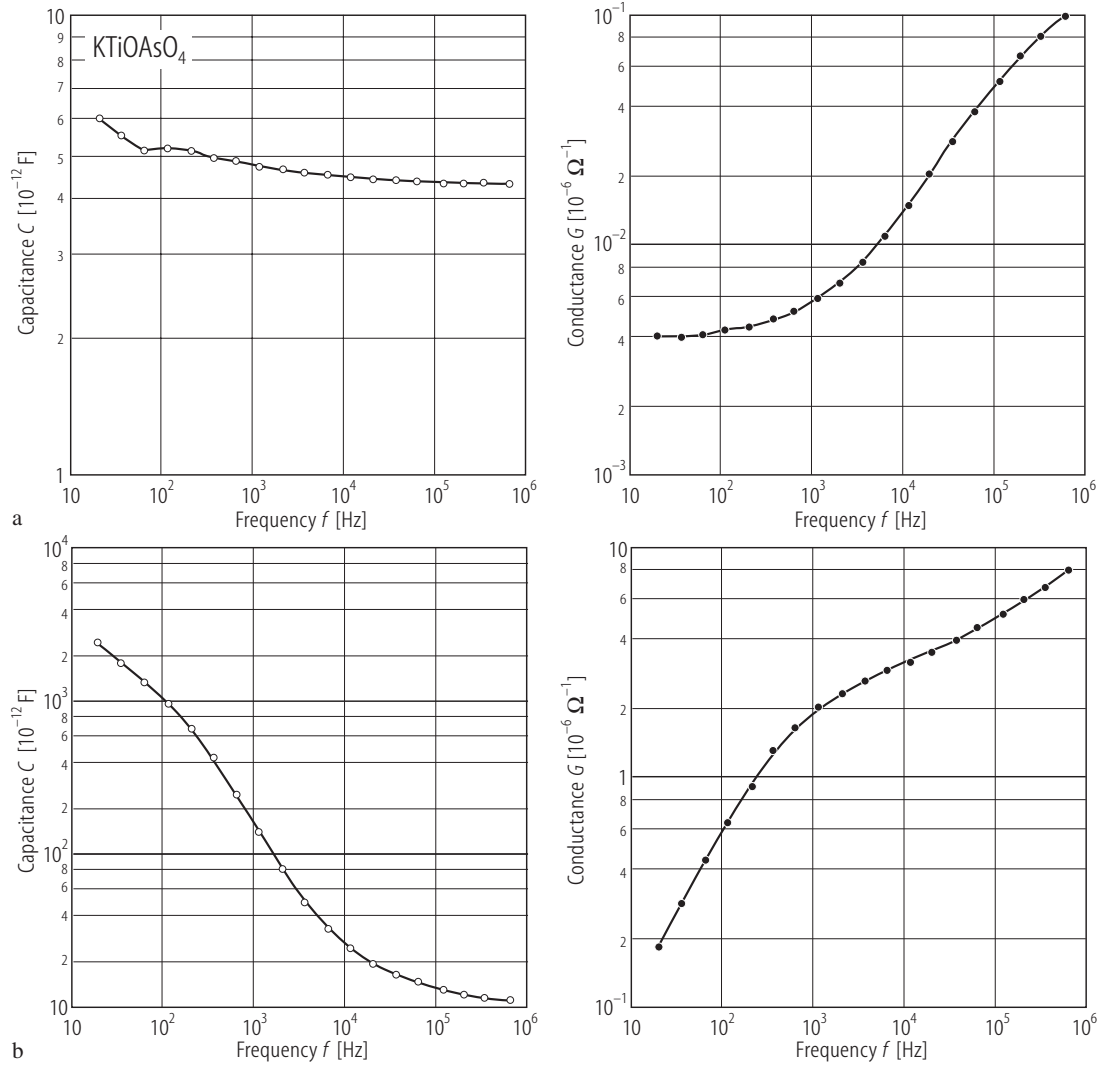


Fig. 35A-20-006. KTiOAsO_4 . C , G vs. f [92Loi2]. C : capacity of the sample. G : conductance. Sample size: $5 \times 5 \times 0.5 \text{ mm}^3$. $T = 22^\circ \text{C}$. (a) [100]; (b) [001].

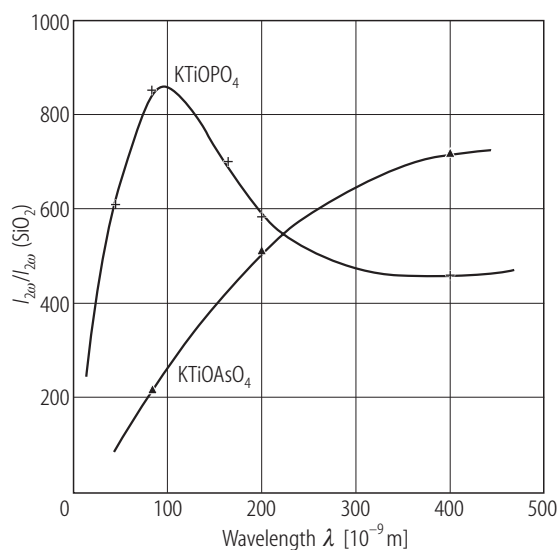


Fig. 35A-20-007. KTiOAsO_4 , KTiOPO_4 . $I_{2\omega}/I_{2\omega}(\text{SiO}_2)$ vs. λ [86EIB]. $I_{2\omega}/I_{2\omega}(\text{SiO}_2)$: ratio of the second harmonic generation to SiO_2 . Powder samples.

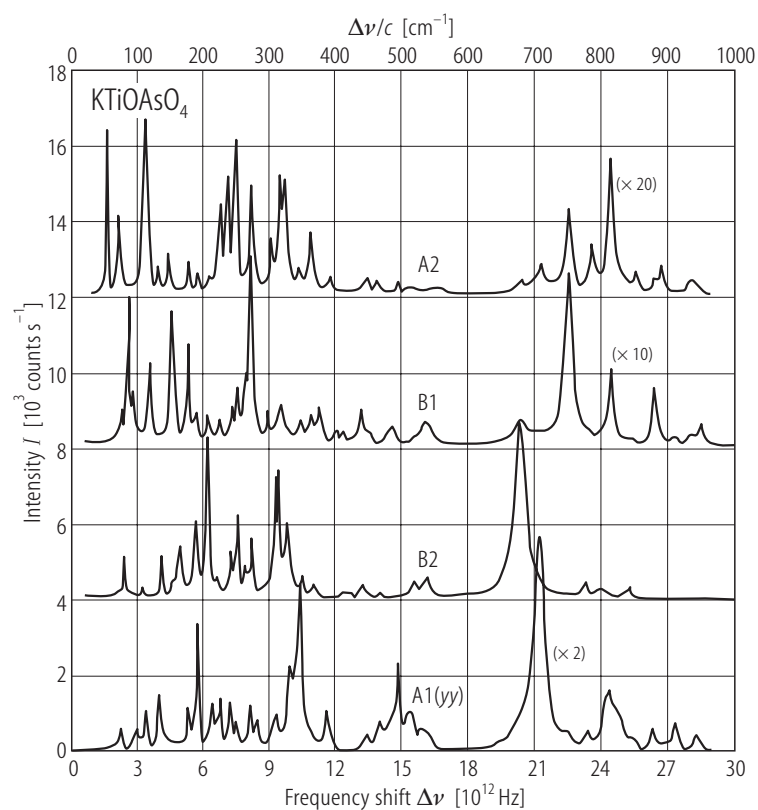


Fig. 35A-20-008. KTiOAsO_4 . I vs. $\Delta\nu$ [91Wat]. I : Raman scattering intensity. $\Delta\nu$: Raman shift.

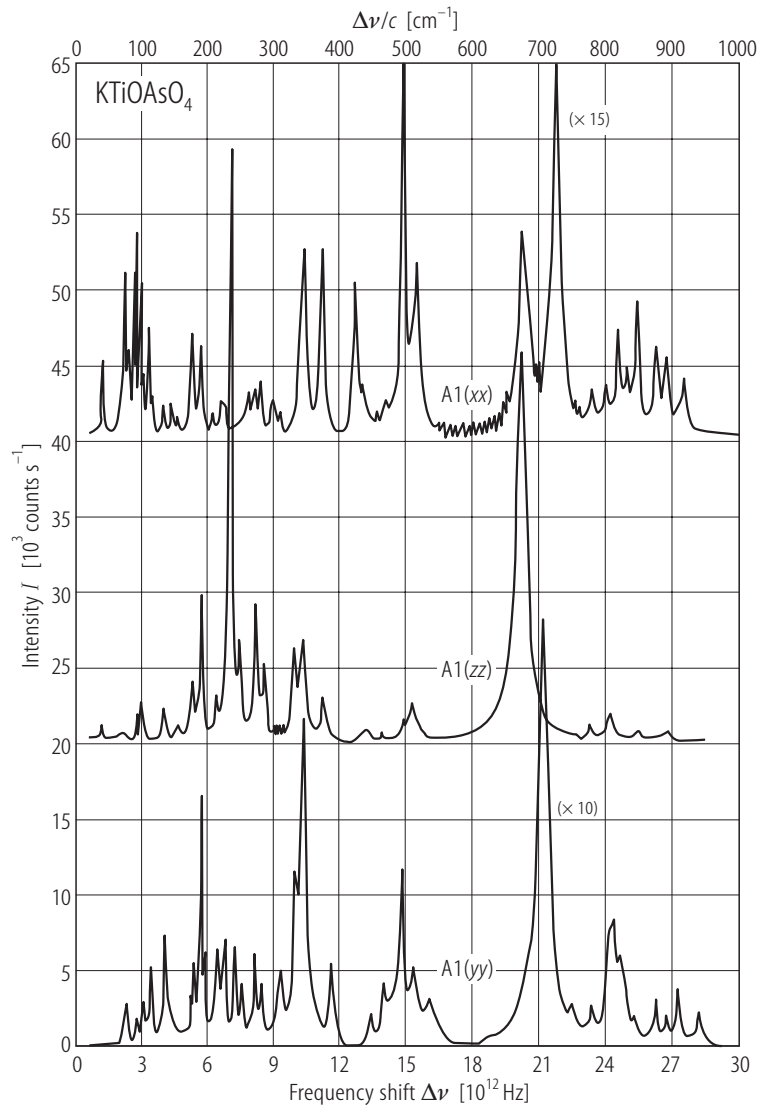


Fig. 35A-20-009. KTiOAsO_4 . I vs. $\Delta\nu$ [91 Wat]. I : Raman scattering intensity. $\Delta\nu$: Raman shift.